Rabi oscillations in an infinite-order correction to the adiabatic approximation for a two-level system

M. E. Crenshaw and C. D. Cantrell
Center for Applied Optics, University of Texas at Dallas, P.O. Box 830688, Richardson, Texas 75083
(Received 9 October 1987)

We derive an infinite-order correction to the adiabatic approximation for the polarization induced in a two-level system by nearly resonant laser irradiation in the low-Rabi-frequency limit for two general classes of field envelopes. We find that Rabi oscillations at the resonant sideband frequency are a general occurrence and study the influence of the pulse shape on the form of the asymptotically decreasing amplitude of the Rabi oscillations as a function of the detuning and time constant. We go beyond the low-Rabi-frequency limit by comparing the analytic solution with numerical solutions of Schrödinger's time-dependent equation. For symmetric laser-pulse envelopes, the numerical solutions predict eigenvalues of the pulse area at which the amplitude of the Rabi oscillations is zero. The phase of the temporal oscillations changes by π at these eigenvalues. For the special case of a hyperbolic-secant envelope, these eigenvalues correspond to the $2n\pi$-area pulses of self-induced transparency. For large-area pulses, the central region of the polarization as a function of time contains additional oscillations, the number of oscillations being determined by the number of pulse-area eigenvalues. For a propagating pulse, these oscillations are impressed on the field and amplified, thereby initiating pulse breakup (nonresonant self-induced transparency).

I. INTRODUCTION

In the adiabatic approximation of quantum mechanics a system remains in an eigenstate of a Hamiltonian of which one or more parameters vary slowly in time.[1-3] The adiabatic approximation is exact in the limit of infinitely slow parametric change. In this limit there are no Rabi oscillations.[1] For any finite rate of change, the system is in a superposition of eigenstates of the instantaneous Hamiltonian, so that the expectation value of an off-diagonal operator such as the dipole moment displays complex oscillations. In this paper we study the dependence of the amplitude and phase of these oscillations on the time history of the Hamiltonian for the specific example of a two-level system irradiated by a laser pulse. The adiabatic approximation discussed here and in Ref. 1 should not be confused with the quasisteady-state approximation in which coherent laser driving is in dynamic equilibrium with collisional and other damping processes.

The results presented here are the foundation for a physical, as well as quantitative, understanding of several coherent laser propagation phenomena. When the contribution of the nonlinear polarization to the laser propagation equation is large compared to the contribution of diffraction, as in many experiments on nearly resonant propagation in atomic vapors, different parts of the wave front propagate nearly independently. In this case the possibly small intensity- and phase-dependent corrections to the adiabatic approximation have a major effect on the evolution of a propagating pulse since these oscillatory corrections are impressed upon the pulse and are amplified in subsequent layers of the medium. We shall describe the application of our results to the explanation of frequency-shifted conical emission in a future publication.[4]

The adiabatic approximation has usefully been applied to problems in the propagation of nearly resonant light in two-level vapors.[5-10] If the field envelope varies slowly compared to the precessional period and if the pulse is sufficiently short that the relaxation times T_1 and T_2' can be considered to be infinite, then the atomic system remains approximately in the quantum-mechanical state that evolves continuously out of the zero-field eigenstate. To the extent that this approximation is valid, no new frequencies are generated. Thus the atomic response can be expressed as a nonlinear dielectric susceptibility, obviating the need for integration of the complete set of quantum-mechanical equations of motion. The adiabatic approximation for the induced polarization in two-level systems was derived phenomenologically by Grischkowsky,[9] who used it to explain certain experimental results of laser propagation. Subsequently, Crisp[3] provided an analytic derivation and obtained an explicit quadrature for the error. We have extended Crisp's results by making a systematic study of the error for a variety of pulse shapes and parameters.

In this paper we derive analytic solutions for an infinite-order near-adiabatic approximation for the induced polarization of an undamped two-level system in the low-Rabi-frequency limit for two general classes of field envelopes. These solutions, which may also be viewed as providing infinite-order corrections to the adiabatic approximation, involve various special functions. For complex arguments the special functions begin oscillating at a finite time and continue to oscillate indefinitely with constant amplitude. We call these the "tail oscillations." From Messiah's discussion of adiabaticity,[2] it is known that the adiabatic approximation is asymptotic. Crisp established its validity for $|\Delta|\tau \gg 1$, where Δ is the detuning from resonance and τ is a characteristic time. The analytic solutions we obtain describe the func-

tional dependence of the asymptotically decreasing amplitude of oscillation on the detuning and time constant. However, the induced polarization contains Rabi oscillations at the resonant sideband frequency $(-\Delta)$ for all finite values of $|\Delta|\tau$.

In the near-adiabatic regime, the infinite-order correction is much smaller than the adiabatic polarization. In order to extend the range of $|\Delta|\tau$ over which nonadiabatic effects are visible in graphs, it is useful to subtract low-order approximations from the total polarization. For this application we derive the first five orders of approximation in Appendix A using a technique introduced by Crisp[3] which does not invoke the low-Rabi-frequency limit. The first two orders of approximation are also derived for a complex field envelope, yielding results that differ from previously published results[3,9] for a real field envelope. The complex formulation is essential in analyzing laser propagation where self-phase modulation causes an initially real field to become complex.

The numerical solution of the two-level time-dependent Schrödinger equation is complicated by imaginary eigenvalues, improper initial conditions (at $t=-\infty$), and adiabaticity requirements. We describe the numerical techniques used to solve Schrödinger's time-dependent equation and compare the numerical solutions with the analytic solutions to show that our infinite-order approximation is valid for a wide range of $|\Delta|\tau$. We then use the numerical method to survey the new effects that occur at higher Rabi frequencies than those to which the analytic solutions apply. For symmetric pulse envelopes, the numerical solutions predict eigenvalues of the pulse area at which the amplitude of the tail oscillations is zero. The phase of the temporal oscillations changes by π at these eigenvalues. For the special case of a hyperbolic-secant envelope, these eigenvalues correspond to the $2n\pi$-area pulses of self-induced transparency. Asymmetric pulses have similar but less sharply defined behavior. For large-area pulses the central region of the polarization (corresponding to the maximum of the incident pulse) contains additional oscillations, the number of oscillations being determined by the number of pulse-area eigenvalues. For a propagating pulse, these oscillations are impressed on the field and amplified, thereby initiating pulse breakup (nonresonant self-induced transparency).

II. COMPLEX POLARIZATION

In this paper we are concerned with the excitation of an ensemble of atoms or molecules with two energy levels connected by an electric dipole transition, the frequency $(\varepsilon/\hbar)$ of which is nearly equal to the laser frequency. In order to make the underlying physics more apparent, we use the undamped time-dependent Schrödinger equation rather than the Bloch equations. This is permitted because the pulse is assumed to be short enough that T_1 and T_2' can be neglected. In the rotating-wave approximation for a system with a ground state and one excited level interacting via an electric dipole transition with an external, classical, time-varying field $E(t)\cos(-\omega t+\phi)$ [where the complex field envelope $E(t)$ is supposed to vary slowly on the time scale of the period $2\pi/\omega$], the time-dependent Schrödinger equation takes the form[1,10]

$$\frac{\partial \bar{c}_0}{\partial t}=i\frac{\mu E(t)^*}{2\hbar}\bar{c}_1 , \tag{1}$$

$$\frac{\partial \bar{c}_1}{\partial t}=i\frac{\mu E(t)}{2\hbar}\bar{c}_0+i\Delta\bar{c}_1 , \tag{2}$$

where Δ is the detuning of the laser frequency from resonance, $\Delta=\omega-\varepsilon/\hbar$; μ is the matrix element of the dipole operator; and $\bar{c}_0$ and $\bar{c}_1$ are the probability amplitudes of the ground state and excited state, respectively. The complex polarization

$$P=2iN\mu\bar{c}_0^*\bar{c}_1 \tag{3}$$

is proportional to the source term of the wave equation describing the spatial propagation of a laser pulse in the slowly varying amplitude and phase approximation.[4,10] The complex polarization is related to the Bloch vector components by $P=iN\mu(u-iv)$. The time derivative of the complex polarization is

$$\frac{dP}{dt}=2iN\mu\left[\bar{c}_0^*\frac{d\bar{c}_1}{dt}+\frac{d\bar{c}_0^*}{dt}\bar{c}_1\right] . \tag{4}$$

Substituting (2) and the conjugate of (1) into (4) and letting $Z=|\bar{c}_1|^2-|\bar{c}_0|^2$ be the inversion results in the first-order linear differential equation

$$\frac{dP}{dt}-i\Delta P=\frac{N\mu^2}{\hbar}EZ , \tag{5}$$

which has the integrating factor $\exp(-i\Delta t)$. With the initial condition $P(-\infty)=0$, the polarization is

$$P(t)=\frac{N\mu^2}{\hbar}\int_{t'=-\infty}^{t'=t}E(t')Z(t')\exp[-i\Delta(t'-t)]dt' . \tag{6}$$

Making the change of variable $x=t-t'$ yields the exact expression

$$P(t)=\frac{N\mu^2}{\hbar}\int_{x=0}^{x=\infty}E(t-x)Z(t-x)\exp(i\Delta x)dx , \tag{7}$$

which is equivalent to a result obtained by Crisp.[3]

Equation (7) is completely general. For a nearly adiabatic pulse, the expression for the inversion derived in Appendix A,[3,9]

$$Z\approx\frac{\pm|\Delta|}{(\Delta^2+\mu^2|E|^2/\hbar^2)^{1/2}} ,$$

can be substituted into the integral. (The minus sign is used for systems starting in the ground state and the plus sign for systems starting in the excited state.) If $\Delta^2\gg\mu^2|E|^2_{\max}/\hbar^2$ (low-Rabi-frequency limit), then the inversion is nearly constant and can be brought outside the integral, resulting in the approximate expression

$$P(t)\approx\frac{N\mu^2Z}{\hbar}\int_{x=0}^{x=\infty}E(t-x)\exp(i\Delta x)dx . \tag{8}$$

For a given field envelope, the integral in Eq. (8) is generally a special function with a complex argument. The technique of solution is to find an integral representation of a special function or a tabulated definite integral that corresponds to (8). To illustrate the method and to de-

scribe the resulting physics we evaluate the integral for the important cases of a generalized Gaussian and a generalized hyperbolic-secant field envelope. Experimentalists often strive to obtain a pulse that is Gaussian in time, while the hyperbolic-secant pulse has long been known to play a special role in the propagation of laser pulses.[11]

Both the Gaussian and the hyperbolic secant are symmetric about a maximum. Real pulses, especially those modified as the result of propagation, may be asymmetric and may have acquired a small modulation at other frequencies than the center frequency ω of the laser pulse. In order to allow for these physically important cases, we multiply the originally symmetric unmodulated pulse envelope by the factor $\exp[(u+iv)t]$. The parameter u allows consideration of asymmetric envelopes such as would occur for a self-steepened pulse. The oscillating component should be thought of as a perturbation of the basic envelope $[1+\varepsilon\exp(ivt)]$, where ε is a real amplitude small compared to 1, rather than an oscillation of the entire envelope. Provided that the amplitude ε is sufficiently small, this allows for an input sideband of nearly arbitrary frequency without violating the adiabatic condition.[1]

III. ANALYTIC SOLUTIONS

A. Gaussian envelope

Consider the generalized Gaussian field envelope

$$E(t)=E_0'\exp[(u+iv)t]\exp\left[-\frac{t^2}{2\tau^2}\right], \tag{9}$$

with u, v, and τ, real, and $\tau>0$. Since the peak of the envelope is located at $t_0=u\tau^2$, we define the normalized amplitude as $E_0'=E_0\exp(-u^2\tau^2/2)$. By Eq. (8), the complex polarization is

$$P(t)\approx\frac{N\mu^2E_0'Z}{\hbar}\int_{x=0}^{x=\infty}\exp[(u+iv)(t-x)]\times\exp\left[-\frac{t^2}{2\tau^2}+\frac{xt}{\tau^2}-\frac{x^2}{2\tau^2}\right]\times\exp(i\Delta x)dx\ . \tag{10}$$

With the subsititutions $\beta=\tau^2/2$ and $\gamma=u-t/\tau^2+i(v-\Delta)$ one converts the integral to

$$P(t)\approx\frac{N\mu^2E_0'Z}{\hbar}\exp\left[-\frac{t^2}{2\tau^2}+(u+iv)t\right]\times\int_{x=0}^{x=\infty}\exp\left[-\frac{x^2}{4\beta}-\gamma x\right]dx\ . \tag{11}$$

In terms of known special functions the result is[12]

$$P(t)\approx\frac{N\mu^2E_0'Z}{\hbar}\exp\left[-\frac{t^2}{2\tau^2}+(u+iv)t\right]\times\sqrt{\pi\beta}\exp(\beta\gamma^2)\mathrm{erfc}(\gamma\sqrt{\beta})\ . \tag{12}$$

The above integral is simply a special case of an integral representation of the parabolic cylinder function.[13]

Because the argument of the complementary error function is complex, the properties of the solution are more apparent if we utilize the so-called complementary error function of complex argument, W, which is defined as[14]

$$W(z)=e^{-z^2}\mathrm{erfc}(-iz)\ . \tag{13}$$

The general solution to (11) becomes

$$P(t)\approx\frac{N\mu^2E_0'Z}{\hbar}\exp\left[-\frac{t^2}{2\tau^2}+(u+iv)t\right]\sqrt{\pi\beta}W(i\gamma\sqrt{\beta})\ , \tag{14}$$

while the polarization for the generalized Gaussian field envelope (9) is

$$P(t)\approx\frac{\tau N\mu^2E_0'Z}{\hbar}\left[\frac{\pi}{2}\right]^{1/2}\exp\left[-\frac{t^2}{2\tau^2}+(u+iv)t\right]\times W\left[\frac{(\Delta-v)\tau}{\sqrt{2}}-i\frac{t-u\tau^2}{\tau\sqrt{2}}\right]\ . \tag{15}$$

The major part of the polarization given by Eq. (15) is a scaled image of the original pulse modified by the complementary error function of complex argument, W.

Because W exhibits smoothly varying behavior if the imaginary part of the argument is positive and complicated behavior if the imaginary part is negative we use the identity[14]

$$W(x-iy)=2\exp(y^2-x^2+2ixy)-[W(x+iy)]^* \tag{16}$$

to divide (15) into a solution valid for $t\le u\tau^2$:

$$P(t)\approx\frac{\tau N\mu^2E_0'Z}{\hbar}\left[\frac{\pi}{2}\right]^{1/2}\exp\left[-\frac{t^2}{2\tau^2}+(u+iv)t\right]\times W\left[\frac{(\Delta-v)\tau}{\sqrt{2}}+i\frac{|t-u\tau^2|}{\tau\sqrt{2}}\right], \tag{17}$$

and a solution valid for $t>u\tau^2$:

$$P(t)\approx\frac{\tau N\mu^2E_0'Z}{\hbar}\sqrt{2\pi}\exp\left[i\Delta t+iu\tau^2(v-\Delta)-\frac{\tau^2}{2}(\Delta^2-2\Delta v+v^2-u^2)\right]-\frac{\tau N\mu^2E_0'Z}{\hbar}\left[\frac{\pi}{2}\right]^{1/2}\exp\left[-\frac{t^2}{2\tau^2}+(u+iv)t\right]\times\left[W\left[\frac{(\Delta-v)\tau}{\sqrt{2}}+i\frac{t-u\tau^2}{\tau\sqrt{2}}\right]\right]^*\ . \tag{18}$$

In order to investigate the most fundamental properties of the solution we consider the symmetric Gaussian envelope by taking $u=v=0$. Perhaps the most interesting feature of the solution is the occurrence of Rabi oscillations at the resonant sideband frequency $(-\Delta)$ beginning at the peak of the envelope, $t=0$, and persisting

indefinitely in time with constant amplitude. The overall phase of these oscillations is the same as the phase of E_0. In this infinite-order low-Rabi-frequency approximation, the amplitude of these oscillations is proportional to $\tau \exp(-\Delta^2\tau^2/2)$, whereas the adiabatic approximation (A19) predicts no oscillations and is valid only if $|\Delta|\tau \gg 1$ (Ref. 3).

Nonzero values of u and v move the peak of the pulse to $u\tau^2$ and introduce a phase factor $\exp[iu\tau^2(v-\Delta)]$ that fixes the node of the Rabi oscillations at the peak. The amplitude of the Rabi oscillations is now proportional to

$$\tau \exp\left[-\frac{\tau^2}{2}(\Delta-v)^2\right]\exp\left[\frac{u^2\tau^2}{2}\right] . \tag{19}$$

For an asymmetric pulse, the amplitude of the tail oscillations depends on the magnitude, but not the sign, of the asymmetry. Constructive interference occurs when v and Δ have the same sign, and destructive interference occurs when they have opposite sign. In particular, if $v=\Delta$ then the amplitude of the Rabi oscillations no longer asymptotically decreases with $\Delta\tau$, but increases with τ for the fraction $\varepsilon/(1+\varepsilon)$ of the pulse that is oscillating initially.

The second term in (18) is also oscillatory when the initial field contains oscillations at frequency v. The complementary error function of complex argument introduces a phase of 0 to $\mathrm{sgn}(\Delta-v)\pi/2$ for $t<u\tau^2$ and from $\mathrm{sgn}(\Delta-v)\pi/2$ to $\mathrm{sgn}(\Delta-v)\pi$ for $t>u\tau^2$. The physically significant result is that during propagation any input sideband oscillations occurring before the peak are amplified and those occurring after the peak are attenuated. The phase approaches the limiting values slowly so that the effect is very small. Further, we have assumed that the fraction of the pulse with input oscillations is small, making the effect much smaller than the tail oscillations resulting from the first term in (18), which operates on the entire pulse envelope.

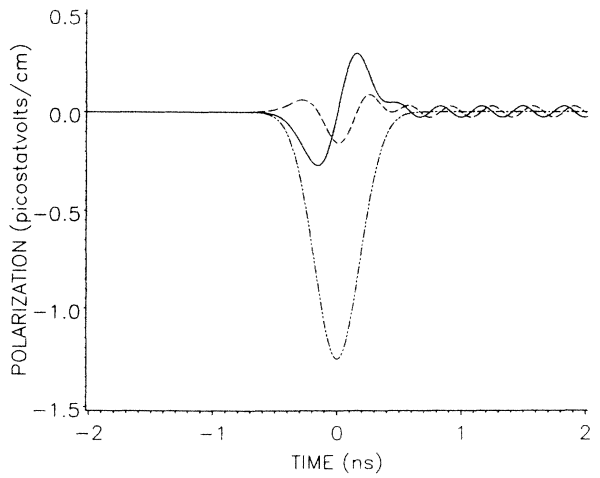

FIG. 1. Polarization for a real, symmetric Gaussian pulse demonstrating the tail Rabi oscillations. The solid line represents the real part of the polarization, the short-dashed–long-dashed line represents the purely imaginary adiabatic polarization, and the dashed line represents the higher-order imaginary polarization. The parameters are $\Delta\bar{\nu}=0.1$ cm^{-1}, $\tau=0.183$ ns, $E_0=50$ statvolts/cm, $\mu=10^{-23}$ statcoulombs cm, and $N=5\times10^{15}$ cm^{-3} ($\bar{\nu}\equiv1/\lambda$).

The result of calculating[15] the polarization from Eqs. (17) and (18) for a real symmetric Gaussian pulse is shown in Fig. 1. The first-order adiabatic polarization (A19) was subtracted from the total polarization in order to make the effects of the higher-order terms more discernible. The tail oscillations are clearly visible in the figure. This figure also shows the asymmetry of the even terms in the expansion which gives rise to pulse reshaping under propagation.

B. Hyperbolic-secant envelope

Consider the generalized hyperbolic-secant field envelope

$$E(t)=E_0'\exp[(u+iv)t]\mathrm{sech}^a(t/\tau) , \tag{20}$$

with a, τ, u, and v real, a and $\tau>0$, and $u>-a/\tau$. If $u<a/\tau$, then the peak of the envelope is located at $t_0=[\ln(1+u\tau/a)-\ln(1-u\tau/a)]\tau/2$. We define the normalized amplitude

$$E_0'=E_0\exp(-ut_0)\cosh^a(t_0/\tau) .$$

By Eq. (8), the complex polarization is

$$P(t)\approx\frac{N\mu^2E_0'Z}{\hbar}\int_{x=0}^{x=\infty}\frac{\exp[(u+iv)(t-x)]}{\cosh^a(t/\tau-x/\tau)}\exp(i\Delta x)dx . \tag{21}$$

Making the exponential substitution for the hyperbolic cosine and defining $z=-\exp(2t/\tau)$, we obtain

$$P(t)\approx\frac{2^aN\mu^2E_0'Z}{\hbar}\exp[(u+a/\tau+iv)t]\times\int_{x=0}^{x=\infty}\frac{\exp\{-[u+a/\tau+i(v-\Delta)]x\}}{[1-z\exp(-2x/\tau)]^a}dx . \tag{22}$$

The change of variable $y=2x/\tau$ and the substitution

$$b=\frac{[u+a/\tau+i(v-\Delta)]\tau}{2} \tag{23}$$

convert (22) to

$$P(t)\approx\frac{2^{a-1}\tau N\mu^2E_0'Z}{\hbar}\exp[(u+a/\tau+iv)t]\times\int_{y=0}^{y=\infty}\frac{\exp(-by)}{[1-z\exp(-y)]^a}dy , \tag{24}$$

which can be expressed as

$$P(t)\approx\frac{2^{a-1}\tau N\mu^2E_0'Z}{\hbar}\exp[(u+a/\tau+iv)t]\left[\frac{1}{b}\right]\times{}_2F_1(a,b;b+1;z) \tag{25}$$

using an integral representation of the hypergeometric function.[16] If $t>0$ then $|z|>1$, and the infinite series

for the hypergeometric function does not converge. However, the function can be evaluated by analytic continuation,[16]

$$ {}_2F_1(a,b;b+1;z)=\frac{b}{b-a}(-z)^{-a} \times {}_2F_1\left[a,a-b;a-b+1;\frac{1}{z}\right] + \frac{b\Gamma(b)\Gamma(a-b)}{\Gamma(a)}(-z)^{-b}, \quad (26) $$

where use has been made of the identity ${}_2F_1(a,0;c;z)=1$. Then the solution is, for $t \leq 0$,

$$ P(t)\approx\frac{2^a\tau N\mu^2E_0'Z}{\hbar}\exp[(u+iv)t]\exp(at/\tau) \times\sum_{n=0}^{\infty}\frac{\Gamma(a+n)}{\Gamma(a)}\frac{(-1)^n\exp(2nt/\tau)}{[a+2n+u\tau+i(v-\Delta)\tau]n!} \quad (27) $$

and for $t>0$,

$$ P(t)\approx\frac{2^a\tau N\mu^2E_0'Z}{\hbar}\exp[(u+iv)t]\exp(-at/\tau) \times\sum_{n=0}^{\infty}\frac{\Gamma(a+n)}{\Gamma(a)}\frac{(-1)^{n+1}\exp(-2nt/\tau)}{[a+2n-u\tau-i(v-\Delta)\tau]n!} + \frac{2^{a-1}\tau N\mu^2E_0'Z}{\hbar}\frac{\Gamma(b)\Gamma(a-b)}{\Gamma(a)}\exp(i\Delta t). \quad (28) $$

The factorials are simplified if we consider only the case where $a=1$. Then the solution is, for $t \leq 0$,

$$ P(t)\approx\frac{2\tau N\mu^2E_0'Z}{\hbar}\exp[(u+iv)t]\exp(t/\tau) \times\sum_{n=0}^{\infty}\frac{(-1)^n\exp(2nt/\tau)}{1+2n+u\tau+i(v-\Delta)\tau} \quad (29) $$

and for $t>0$,

$$ P(t)\approx\frac{2\tau N\mu^2E_0'Z}{\hbar}\exp[(u+iv)t]\exp(-t/\tau) \times\sum_{n=0}^{\infty}\frac{(-1)^{n+1}\exp(-2nt/\tau)}{1+2n-u\tau-i(v-\Delta)\tau} + \frac{\tau N\mu^2E_0'Z}{\hbar}\exp(i\Delta t)\pi \times\operatorname{sech}\left[\frac{\pi\tau(v-\Delta)}{2}-\frac{iu\tau\pi}{2}\right]. \quad (30) $$

The physical properties of this solution have much in common with the results given for the Gaussian pulse. The polarization contains Rabi oscillations at the resonant sideband frequency that begin at a finite time and continue indefinitely with constant amplitude. The oscillations have an amplitude that is an exponentially decreasing function of $|\Delta|\tau$ and which demonstrates constructive or destructive interference with an input sideband. The phase ϕ of the oscillations is determined by the phase of E_0 and by the asymmetry constant u through the expression

$$ \tan(\phi)=\tanh\left[\frac{\pi\tau(v-\Delta)}{2}\right]\tan\left[\frac{u\tau\pi}{2}\right]. \quad (31) $$

The magnitude of the oscillations is proportional to

$$ \tau\left[\cosh^2\left[\frac{\pi\tau(v-\Delta)}{2}\right]-\sin^2\left[\frac{u\tau\pi}{2}\right]\right]^{-1/2}, \quad (32) $$

which again depends on the magnitude, but not the sign, of the asymmetry constant u.

An important special case of the input pulse (20) occurs when $a=1$ and $u=1/\tau$. The pulse shape is then a Fermi pulse and the oscillation magnitude becomes proportional to $|\tau\operatorname{csch}[\pi\tau(v-\Delta)/2]|$, which asymptotically approaches ∞ as the argument approaches zero, demonstrating considerable interference between the Rabi oscillations and the input sideband.

Figure 2 shows real hyperbolic-secant pulses with positive ($u=+2.1$) and negative ($u=-2.1$) asymmetry. Equations (29) and (30) were evaluated for these pulses. In both cases, the first-order adiabatic polarization was subtracted from the total polarization in order to make the effects of the higher-order terms more discernible. The results are shown in Fig. 3 for the positive-asymmetry case and in Fig. 4 for the negative-asymmetry case, where the solid line is the real polarization and the dashed line is the higher-order imaginary polarization. The purely imaginary, first-order adiabatic polarization, which is not shown, is an inverted image of the electric field with magnitude 1.26 picostatvolts/cm.

IV. NUMERICAL METHOD

In this section we describe the numerical method used to solve the time-dependent Schrödinger equation [Eqs.

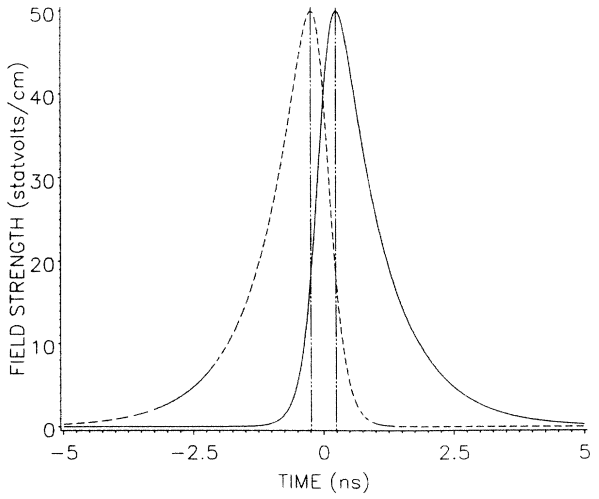

FIG. 2. Hyperbolic-secant pulses with positive (solid line) and negative (dashed line) asymmetry. The parameters are $\tau=0.31$ ns, $E_0=50$ statvolts/cm, and $u=\pm 2.1$.

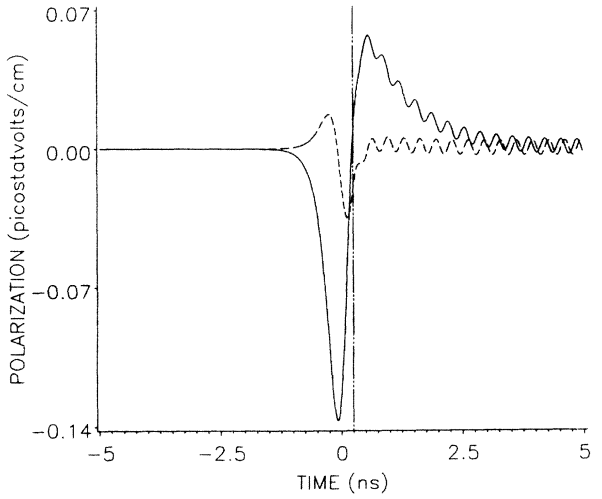

FIG. 3. Polarization for the real, positive asymmetry, hyperbolic-secant pulse shown in Fig. 2. The solid line represents the real part of the polarization and the dashed line represents the higher-order imaginary polarization. The parameters are $\Delta\bar{\nu}=0.1$ cm^{-1}, $\mu=10^{-23}$ statcoulombs cm, and $N=5\times10^{15}$ cm^{-3}.

(1) and (2)] in order to verify the applicability of the analytic solutions which were derived assuming near-adiabaticity and low-Rabi-frequency limit, and to extend the solution beyond the range of validity of the adiabatic and low-Rabi-frequency approximations. The most significant aspect of the differential equations (1) and (2), from a numerical point of view, is that they have imaginary eigenvalues. Because of these imaginary eigenvalues, it is surprisingly difficult to obtain *accurate* numerical solutions for an arbitrary time-dependent field envelop $E(t)$. Several well-known methods for solving systems of ordinary differential equations are actually unstable for equations with purely imaginary eigenvalues. Chu and Cantrell[17] present a method for solving the time-dependent Schrödinger equation that has a very small local error and high computational speed. The finite-difference equations for their multistep method are

$$y_{n+1}=0.43y_n-0.35y_{n-2}+0.92y_{n-3}+2.38hy'_n -1.59hy'_{n-1}+2.28hy'_{n-2}-0.01hy'_{n-3}\ , \tag{33}$$

with a stability limit of $0.6i$. For the numerical results presented here, the multistep finite-difference method was started with an Euler predictor and an iterated trapezoidal corrector. This starter is stable but is not suitable for the complete solution due to the amount of iteration required to achieve acceptable accuracy.

At the end of the numerical calculations it is necessary to verify the accuracy of the solution by calculating the norm of the state vector $|\bar{c}_0|^2+|\bar{c}_1|^2$, which must be unity to within a prescribed error range. A standard technique for determining the required accuracy of a finite-difference method is to compare the solution for a given step size with the solution for a half-step size. The error range $0.9999\leq|\bar{c}_0|^2+|\bar{c}_1|^2\leq1.0001$ was consistent with repeatable results when a smaller step size was used. Due to small-scale structure at the generalized Rabi frequency,

$$\Omega'(t)=(\Delta^2+\mu^2|E(t)|^2/\hbar^2)^{1/2}\ , \tag{34}$$

the number of time points required to achieve this level of accuracy was often considerably greater than the Nyquist limit based on the detuning frequency alone. We note that this physical structure is present in the total polarization when $|\Delta|\tau$ is large, but may not be visible graphically. Techniques that can be used to make it visible include subtraction of the low-order polarization (Appendix A) and truncation of larger features. The origin and characteristics of this small-scale, high-frequency structure are discussed in Sec. V.

An additional numerical difficulty is the imposition of an initial value that is defined at $t=-\infty$. Since the field varies slowly from $t=-\infty$ to the point where the calculations begin, we can use the dressed state (eigenstate of the effective Hamiltonian) that is correlated with the initial zero-field state as the initial value for solving Eqs. (1) and (2), provided the logarithmic derivative of E is also small.[1] In order to meet the second part of the adiabatic criterion, which limits the logarithmic derivative of $E(t)$, a small field of constant amplitude, which we call a pedestal, is added to the field.

For the system of Eqs. (1) and (2), the effective Hamiltonian is given by

$$H^{\text{eff}}=\begin{bmatrix}0 & \Omega^* \\ \Omega & \Delta\end{bmatrix}\ , \tag{35}$$

where $\Omega=\mu E/2\hbar$. The eigenvalue of (35) corresponding to the ground state is

$$\lambda_0=\frac{\Delta}{2}\left[1-\left[1+4\frac{|\Omega|^2}{\Delta^2}\right]^{1/2}\right]\ , \tag{36}$$

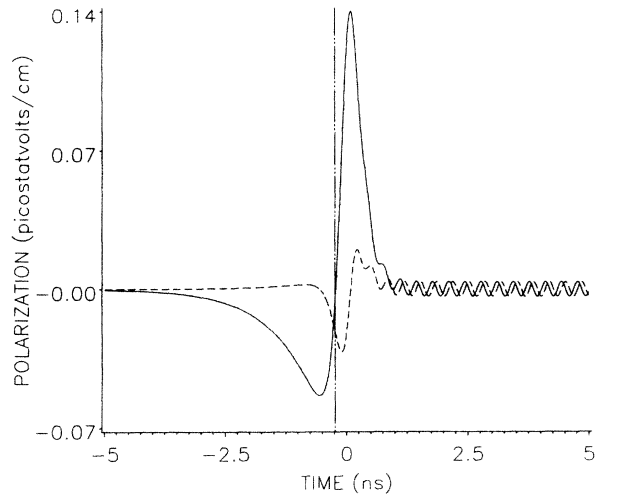

FIG. 4. Polarization for the real, negative asymmetry, hyperbolic-secant pulse shown in Fig. 2. The solid line represents the real part of the polarization and the dashed line represents the higher-order imaginary polarization. The parameters are the same as for Fig. 3.

and a corresponding normalized dressed-state eigenvector is

$$\tilde{c}_1 = \left[\frac{\lambda_0^2}{|\Omega|^2 + \lambda_0^2} \right]^{1/2}, \tag{37}$$

$$\tilde{c}_0 = \frac{\tilde{c}_1 \Omega^*}{\lambda_0} . \tag{38}$$

Due to a small amount of nonadiabaticity, the system is not precisely in the dressed state (37) and (38). It is therefore necessary to start the calculations when the field is quite small and almost constant in order to allow the parasitic roots of the finite-difference method[17] to die away before the field becomes significant. The derivative of the phase of a propagated field is used as a sensitive indicator to verify that the calculations were started adiabatically. If the derivative of the phase is not smooth, then the parasitic roots have not died off rapidly enough and the physical small-scale structure may have been lost, even though the accuracy criterion has been met.

V. NUMERICAL RESULTS

The finite-difference solution of Schrödinger's equation described in Sec. IV was used to test the validity of the analytic solutions and to extend these results to higher intensities. For all numerical calculations, the system was started in the ground state and the pedestal was 5×10^{-3} statvolts/cm (intensity $=3\times10^{-6}$ kW/cm^2).

The analytic solutions (17) and (18), and (29) and (30), were evaluated numerically and compared with the finite-difference solutions. A dipole moment of 10^{-23} statcoulombs cm [compared to 6.49×10^{-18} statcoulombs cm for the $(3\,^2S_{1/2}-3\,^2P_{3/2})D_2$ transition of Na] and a field strength of 50 statvolts/cm (intensity $=300$ kW/cm^2) were chosen as a representative of the low-Rabi-frequency limit. In order to facilitate comparisons, the first-order adiabatic polarization (A19) was subtracted from the total polarization. No discernible difference was found between the finite-difference solution and the analytic solutions over the entire range of parameters tested, except near the origin, where, for certain ranges of the parameters, the infinite series in Eqs. (29) and (30) did not converge sufficiently fast. The range of $\Delta\tau$ was from 5.00, where the Rabi oscillations were barely observable, to 0.001, where the oscillations dominate the higher-order polarization.

For values of μE_0 that violate the low-Rabi-frequency limit considered in the previous paragraph, the finite-difference and analytic solutions begin to diverge. The frequency of oscillation was investigated for positive asymmetry pulses where the generalized Rabi frequency decreases slowly from $(\Delta^2+\mu^2E_0^2/\hbar^2)^{1/2}$ at the peak of the pulse, asymptotically approaching Δ at large time. It was found that the oscillations occur at the instantaneous generalized Rabi frequency.

The finite-difference solution to Schrödinger's equation was also used to make a systematic study of the variation in the amplitude of the tail oscillations for larger intensities. A parameter of interest is the pulse area, which is important in pulse propagation[11] and is proportional to μE_0. The pulse area Θ, defined as the angle through which the pseudodipole rotates during the pulse when the detuning is zero, is given by the expression

$$\Theta = \int_{t=-\infty}^{t=\infty} \frac{\mu E(t)}{\hbar} dt . \tag{39}$$

For symmetric pulses, there exist eigenvalues of pulse area at which the amplitude of the tail oscillations is zero. For resonant pulses, these eigenvalues occur at a pulse area of $2n\pi$, where the pseudodipole makes n complete revolutions and the medium is returned to its initial state. For nonresonant pulses, the pulse-area eigenvalues depend on the pulse shape; the pulse area must be such that the energy absorbed during the rise of the pulse is reemitted into the tail at a rate that exactly follows the fall of the pulse. If there are no tail oscillations, then no energy remains in the medium after the pulse has passed.

The hyperbolic-secant pulse is a special case where the eigenvalues of the pulse area at which the amplitude of the oscillations is zero occur at integer multiples of 2π for *all* values of detuning and time constant. The eigenvalues of a symmetric, Gaussian pulse exhibit more complex behavior. Figure 5 shows the variation of the first few eigenvalues with Δ. Only positive detunings are shown since the eigenvalues are symmetric about the resonance. For small Δ, the pulse-area eigenvalues asymptotically approach the $2n\pi$ area expected for resonance. For nonzero detuning, the eigenvalues also approach $2n\pi$ asymptotically with decreasing τ.

Figure 6 shows plots of the oscillation amplitude (zero to peak of the out-of-phase quadrature) versus E_0 for several values of asymmetry of a real hyperbolic-secant pulse. The dashed line corresponding to a very small asymmetry is visible as a rounding of the cusps of the amplitude, displaying the sensitivity of the eigenvalue behavior to asymmetry. In Fig. 7 we present the phase of the oscillation as a function of E_0 for the same pulses. The

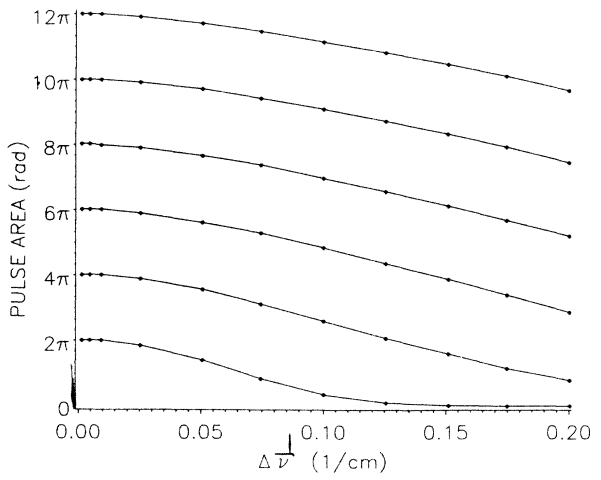

FIG. 5. Eigenvalues of pulse area, as μ is varied, as a function of detuning for a real, symmetric, Gaussian pulse. The eigenvalues are symmetric with respect to the detuning. The parameters are $\tau=0.212$ ns, $E_0=50$ statvolts/cm, and $N=5\times10^{15}$ cm^{-3}.

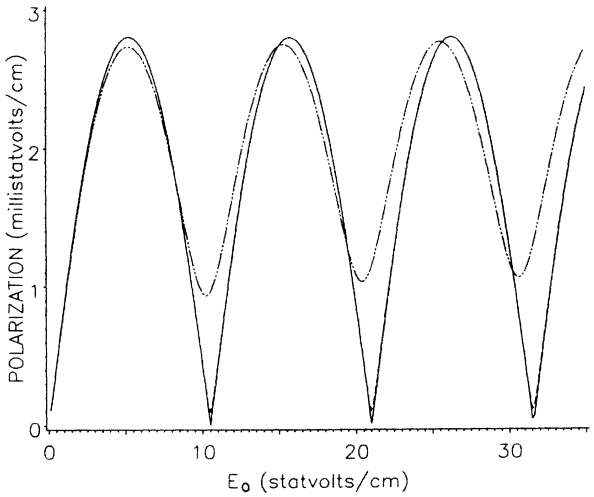

FIG. 6. Amplitude of Rabi oscillations in the polarization as a function of E_0 for five values of asymmetry for a real hyperbolic-secant pulse. The values of u are $u=0.0$ (solid line), $u=\pm 0.1$ (dashed line), and $u=\pm 1.0$ (short-dashed–long-dashed line). Additional parameters: $N=5\times 10^{15}$ cm^{-3}, $\mu=10^{-18}$ statcoulombs cm, $\tau=0.2$ ns, and $\Delta\bar{\nu}=0.032$ cm^{-1}.

eigenvalues of the Schrödinger equation discussed here are distinct from the bound-state eigenvalues of the coupled Maxwell-Bloch equations[18] which determine the asymptotic result of uniform plane-wave propagation.

In the nearly adiabatic regime, the pseudodipole precesses in a narrow cone about the slowly evolving effective field (torque vector) in Bloch space.[19] This precession induces oscillations in the polarization, with an asymptotically small amplitude, at the instantaneous generalized Rabi frequency. When the torque vector changes its direction very slowly compared with the rate of precession, the trajectory of the tip of the pseudodipole is approximately equivalent to rotation in a plane. Further, the plane of rotation must slowly change its orientation in order to remain perpendicular to the torque vector. For nonresonant pulses, the oscillations in the polarization have both in-phase and out-of-phase components because the plane of rotation is not parallel to the v-z plane in Bloch space. An example is shown in Fig. 8, where the oscillations are made visible by subtracting out the fifth-order approximation (A35) to the polarization. The ratio of the amplitude of the imaginary component of the oscillations to the amplitude of the real component is given by the absolute value of the sine of the angle between the effective field and the u axis,

$$\frac{A_i}{A_r}=\frac{|\Delta|}{\{\Delta^2+4[\Omega(t)]^2\}^{1/2}} . \tag{40}$$

When viewed from the origin, the pseudodipole rotates clockwise about the torque vector. The oscillating portions of the Bloch vector components are

$$u_{\rm osc}=-\mathrm{sgn}(\Delta)A_i\cos(\Omega' t) \tag{41}$$

and

$$v_{\rm osc}=A_r\sin(\Omega' t) . \tag{42}$$

The complex polarization $P=iN\mu(u-iv)$ becomes

$$P=P_0-\frac{iN\mu A_r}{2}\left[\left[1+\frac{\Delta}{\Omega'}\right]e^{i\Omega' t}-\left[1-\frac{\Delta}{\Omega'}\right]e^{-i\Omega' t}\right] , \tag{43}$$

where P_0 is the contribution of the nonoscillating components due to the evolution of the effective field. From this equation we see that the sideband on the resonance side of the center frequency is larger than the opposite sideband for nonresonant pulses.

The central oscillations are the origin of pulse breakup

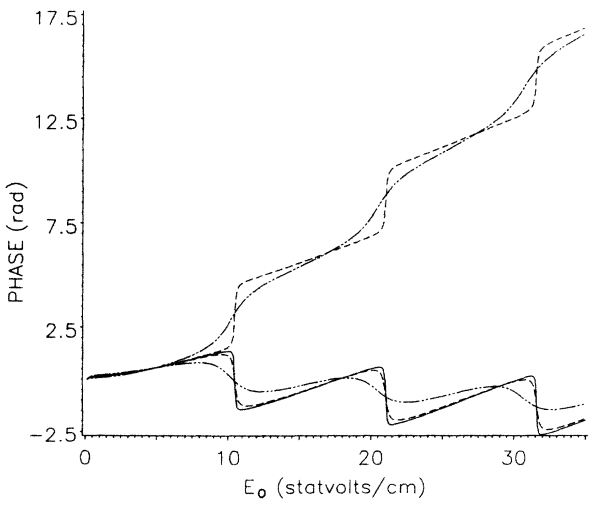

FIG. 7. Phase of the Rabi oscillations as a function of E_0 for five values of asymmetry for the same pulse as Fig. 6. The values of u are $u=0.0$ (solid line), $u=0.1$ (upper dashed line), $u=1.0$ (upper short-dashed–long-dashed line), $u=-0.1$ (lower dashed line), and $u=-1.0$ (lower short-dashed–long-dashed line).

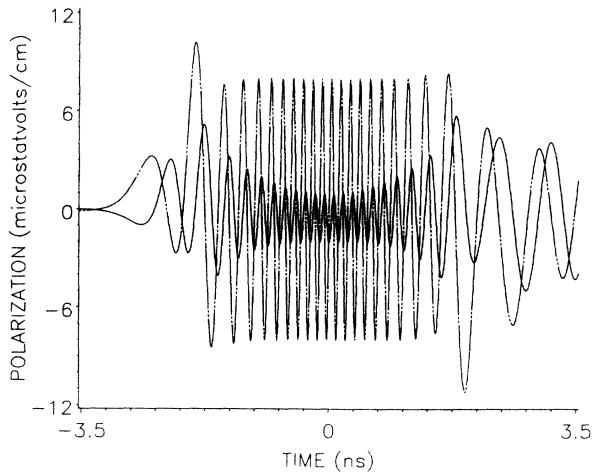

FIG. 8. Higher-order real (dashed line) and imaginary (solid line) polarization for a real, symmetric Gaussian pulse demonstrating relative amplitudes of the central oscillations. The parameters are $\Delta\bar{\nu}=0.0478$ cm^{-1}, $\tau=1.06$ ns, $E_0=50$ statvolts/cm, $\mu=10^{-18}$ statcoulombs cm, and $N=5\times 10^{15}$ cm^{-3}.

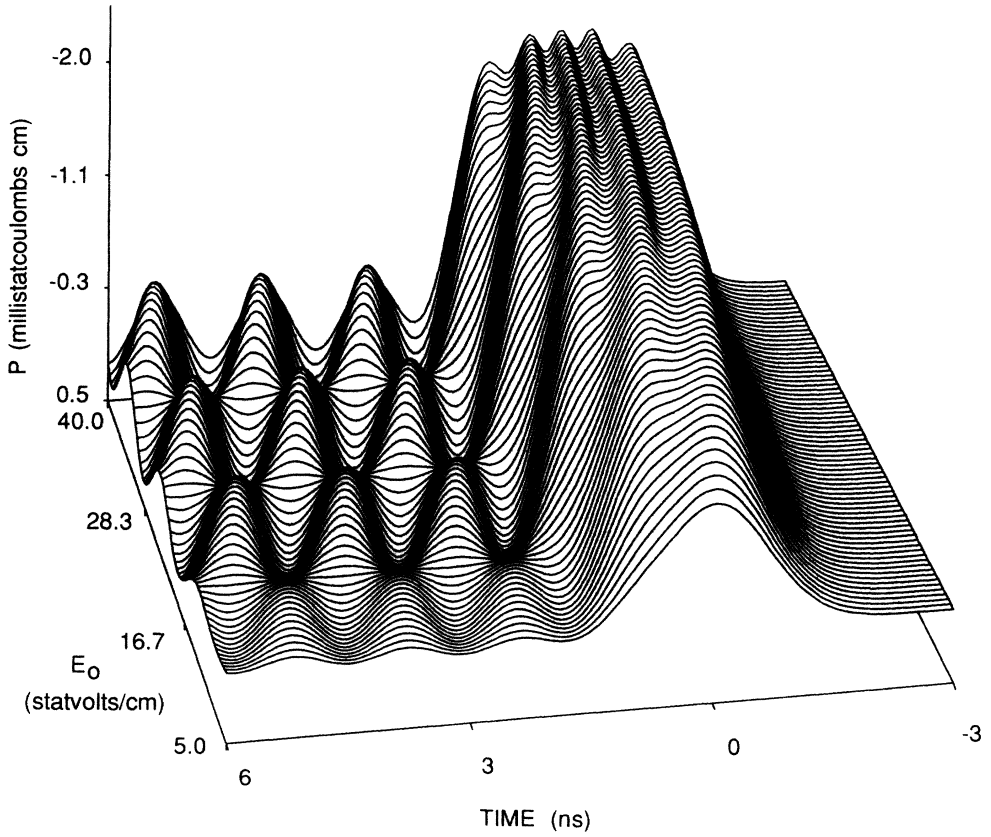

FIG. 9. Polarization as a function of E_0 for a real, symmetric Gaussian pulse demonstrating addition of lobes at the pulse-area eigenvalues. The polarization axis is inverted to expose features. The parameters are $\Delta\bar{\nu}=0.0239$ cm^{-1}, $\tau=0.743$ ns, $\mu=4\times10^{-19}$ statcoulombs cm, and $N=5\times10^{15}$ cm^{-3}.

into subpulses. A lobe is added to the polarization for each eigenvalue of pulse area, as shown in Fig. 9. As the pulse propagates the oscillations in the polarization are impressed on the field and then amplified by several mechanisms, including those discussed in Sec. III. The rate at which pulse breakup develops depends strongly on Δ and τ in accordance with the amplitude of the central oscillations.

VI. SUMMARY

The analytic solutions for the infinite-order near-adiabatic polarization explicitly detail the manner in which physical phenomena develop from the adiabatic limit for low-Rabi-frequency pulses. In addition, they are a useful starting point for determining how near-adiabatic effects are affected by the Rabi frequency and what additional effects develop that are not contained in the near-adiabatic, low-Rabi-frequency limit.

ACKNOWLEDGMENTS

The authors wish to thank K. Strozewski for assistance with data acquisition and computer graphics. This research was supported by Cray Research, Inc., Convex Computer Corporation, the U.S. Office of Naval Research, the National Science Foundation, the Texas Advanced Technology and Research Program, and the University of Texas System Center for High Performance Computing.

APPENDIX A

The derivation of the adiabatic approximation by integrating the polarization integral (6) by parts is due to Crisp,[3] who derived the first-order approximation to the inversion and two orders of approximation to the polarization for real field envelopes. In this appendix, expressions for the first-order through fifth-order approximations to the inversion and polarization are derived for real field envelopes. Making higher-order approximations to the inversion, as well as the polarization, results in a significant improvement in the accuracy of this approximation technique. First- and second-order approximations to the inversion and polarization are also derived for complex field envelopes. The complex formulation is essential in analyzing laser propagation where self-phase modulation causes an initially real field to become complex. In what follows the subscript (n) is used to indicate the order of the approximation of the inversion Z and the polarization P; unsubscripted variables imply the exact expression. Repeatedly integrating the polarization integral (6) by parts, defining the radiative coupling $\Omega=\mu E/2\hbar$, and dividing by $2iN\mu$ results in an expression for $\bar{c}_0^*\bar{c}_1$:

$$\tilde{c}_0^*\tilde{c}_1=\frac{\Omega Z}{\Delta}-\frac{i}{\Delta^2}\frac{d(\Omega Z)}{dt}-\frac{1}{\Delta^3}\frac{d^2(\Omega Z)}{dt^2}+\frac{i}{\Delta^4}\frac{d^3(\Omega Z)}{dt^3}+\frac{1}{\Delta^5}\frac{d^4(\Omega Z)}{dt^4}+\cdots . \tag{A1}$$

Allowing for a complex field, the derivatives

$$\frac{dZ}{dt}=2i(\Omega\tilde{c}_0\tilde{c}_1^*-\Omega^*\tilde{c}_0^*\tilde{c}_1) , \tag{A2}$$

$$\frac{d(\tilde{c}_0^*\tilde{c}_1)}{dt}=-i(\Omega Z-\Delta\tilde{c}_0^*\tilde{c}_1) , \tag{A3}$$

and

$$\frac{d(\tilde{c}_0\tilde{c}_1^*)}{dt}=+i(\Omega^*Z-\Delta\tilde{c}_0\tilde{c}_1^*) \tag{A4}$$

are obtained by using the time-dependent Schrödinger equation to eliminate the derivatives of the Schrödinger coefficients. Specializing to a purely real field and using Eqs. (A2)–(A4) to eliminate derivates of the inversion, the terms of the expansion (A1) are recast in terms of the inversion and the Schrödinger coefficients:

$$-\frac{i}{\Delta^2}\frac{d(\Omega Z)}{dt}=-\frac{i}{\Delta^2}\frac{d\Omega}{dt}Z-\tilde{c}_0^*\tilde{c}_1\left[\frac{2\Omega^2}{\Delta^2}\right]+\tilde{c}_0\tilde{c}_1^*\left[\frac{2\Omega^2}{\Delta^2}\right] , \tag{A5}$$

$$-\frac{1}{\Delta^3}\frac{d^2(\Omega Z)}{dt^2}=Z\left[\frac{4\Omega^3}{\Delta^3}-\frac{1}{\Delta^3}\frac{d^2\Omega}{dt^2}\right]+\tilde{c}_0^*\tilde{c}_1\left[-\frac{2\Omega^2}{\Delta^2}+i\frac{6\Omega}{\Delta^3}\frac{d\Omega}{dt}\right]+\tilde{c}_0\tilde{c}_1^*\left[-\frac{2\Omega^2}{\Delta^2}-i\frac{6\Omega}{\Delta^3}\frac{d\Omega}{dt}\right] , \tag{A6}$$

$$+\frac{i}{\Delta^4}\frac{d^3(\Omega Z)}{dt^3}=iAZ+\tilde{c}_0^*\tilde{c}_1(-B+iC)+\tilde{c}_0\tilde{c}_1^*(B+iC) , \tag{A7}$$

and

$$+\frac{1}{\Delta^5}\frac{d^4(\Omega Z)}{dt^4}=DZ+\tilde{c}_0^*\tilde{c}_1(F+iG)+\tilde{c}_0\tilde{c}_1^*(F-iG) . \tag{A8}$$

The temporary variables are defined as follows:

$$A=-\frac{24\Omega^2}{\Delta^4}\frac{d\Omega}{dt}+\frac{1}{\Delta^4}\frac{d^3\Omega}{dt^3} , \tag{A9}$$

$$B=\frac{2\Omega^2\Omega'^2}{\Delta^4}-\frac{6}{\Delta^4}\left[\frac{d\Omega}{dt}\right]^2-\frac{8\Omega}{\Delta^4}\frac{d^2\Omega}{dt^2} , \tag{A10}$$

$$C=\frac{10\Omega}{\Delta^3}\frac{d\Omega}{dt} , \tag{A11}$$

$$D=\frac{4\Omega^3\Omega'^2}{\Delta^5}-\frac{60\Omega}{\Delta^5}\left[\frac{d\Omega}{dt}\right]^2-\frac{40\Omega^2}{\Delta^5}\frac{d^2\Omega}{dt^2}+\frac{1}{\Delta^5}\frac{d^4\Omega}{dt^4} , \tag{A12}$$

$$F=-\frac{2\Omega^2\Omega'^2}{\Delta^4}+\frac{16}{\Delta^4}\left[\frac{d\Omega}{dt}\right]^2+\frac{18\Omega}{\Delta^4}\frac{d^2\Omega}{dt^2} , \tag{A13}$$

and

$$G=\frac{14\Omega}{\Delta^3}\frac{d\Omega}{dt}+\frac{80\Omega^3}{\Delta^5}\frac{d\Omega}{dt}-\frac{20}{\Delta^5}\frac{d\Omega}{dt}\frac{d^2\Omega}{dt^2}-\frac{10\Omega}{\Delta^5}\frac{d^3\Omega}{dt^3} , \tag{A14}$$

where Ω' is the (instantaneous) generalized Rabi frequency $\Omega'(t)=\{\Delta^2+4[\Omega(t)]^2\}^{1/2}$.

The first-order (adiabatic) approximation consists of assuming that the field and inversion vary slowly such that only the first term in the expansion (A1) is significant:

$$\tilde{c}_0^*\tilde{c}_1\approx\frac{\Omega Z_{(1)}}{\Delta} . \tag{A15}$$

Multiplying the previous equation by the complex-conjugate equation and by 4 yields

$$4|\tilde{c}_0|^2|\tilde{c}_1|^2\approx\frac{4\Omega^2}{\Delta^2}Z_{(1)}^2 . \tag{A16}$$

Expanding Z^2 in terms of the Schrödinger probability amplitudes and adding it to both sides of the previous equation, one obtains

$$|\tilde{c}_0|^4+2|\tilde{c}_0|^2|\tilde{c}_1|^2+|\tilde{c}_1|^4\approx\frac{4\Omega^2}{\Delta^2}Z_{(1)}^2+Z^2 . \tag{A17}$$

The left-hand side of the preceding equation is $(|\tilde{c}_0|^2+|\tilde{c}_1|^2)^2=1$. Making the approximation $Z\approx Z_{(1)}$ and solving for $Z_{(1)}$ results in the usual expression for the inversion in the adiabatic approximation,[3,9]

$$Z_{(1)}\approx\pm\frac{1}{\left[1+\frac{4\Omega^2}{\Delta^2}\right]^{1/2}}=\pm\left|\frac{\Delta}{\Omega'}\right| . \tag{A18}$$

In Eq. (A18), and all subsequent equations for the inversion, the negative sign is appropriate for a system starting from the ground state at $t=-\infty$ (attenuator) and the positive sign is appropriate for a system starting in the excited state (amplifier). The first-order (adiabatic) polarization is simply Eq. (A15) multiplied by $2iN\mu$:

$$P_{(1)}=\frac{2iN\mu\Omega Z_{(1)}}{\Delta} . \tag{A19}$$

The second-order approximation consists of the first two terms on the right-hand side of (A1). Making the approximations $Z\approx Z_{(2)}$ and $(dZ/dt)\approx(dZ_{(2)}/dt)$ allows Eq. (A5) to be used for the second term:

$$\tilde{c}_0^*\tilde{c}_1\approx Z_{(2)}\left[\frac{\Omega}{\Delta}-\frac{i}{\Delta^2}\frac{d\Omega}{dt}\right]-\tilde{c}_0^*\tilde{c}_1\frac{2\Omega^2}{\Delta^2}+\tilde{c}_0\tilde{c}_1^*\frac{2\Omega^2}{\Delta^2} . \tag{A20}$$

Grouping coefficients of $\tilde{c}_0^* \tilde{c}_1$ and using the complex conjugate of the resulting equation to eliminate $\tilde{c}_0 \tilde{c}_1^*$ gives

$$\tilde{c}_0^* \tilde{c}_1 \left[1+\frac{4\Omega^2}{\Delta^2} \right] \approx Z_{(2)} \left[\frac{\Omega}{\Delta} \left[1+\frac{4\Omega^2}{\Delta^2} \right] - \frac{i}{\Delta^2} \frac{d\Omega}{dt} \right] . \tag{A21}$$

Multiplying by the complex-conjugate equation and by 4, expanding Z^2 in terms of the Schrödinger probability amplitudes and adding it to both sides of the resulting equation, making the approximation $Z \approx Z_{(2)}$, and solving for $Z_{(2)}$ yields

$$Z_{(2)} \approx \pm \left| \frac{\Delta}{\Omega'} \right| \left[1+\frac{4\Delta^2}{\Omega'^6} \left[\frac{d\Omega}{dt} \right]^2 \right]^{-1/2} . \tag{A22}$$

The second-order polarization

$$P_{(2)} = 2iN\mu Z_{(2)} \left[\frac{\Omega}{\Delta} - \frac{i}{\Omega'^2} \frac{d\Omega}{dt} \right] \tag{A23}$$

is obtained from Eq. (A21).

In the next order of approximation, the first three terms on the right-hand side of (A1) are used. Making the approximations $Z \approx Z_{(3)}$, $(dZ/dt) \approx (dZ_{(3)}/dt)$, and $(d^2Z/dt^2) \approx (d^2Z_{(3)}/dt^2)$, and using Eqs. (A5) and (A6) to eliminate the derivatives of the inversion, one obtains

$$\begin{aligned} \tilde{c}_0^* \tilde{c}_1 \approx Z_{(3)} & \left[\frac{\Omega}{\Delta} \left[1+\frac{4\Omega^2}{\Delta^2} \right] - \frac{1}{\Delta^3} \frac{d^2\Omega}{dt^2} - \frac{i}{\Delta^2} \frac{d\Omega}{dt} \right] \\ & - \tilde{c}_0^* \tilde{c}_1 \left[\frac{4\Omega^2}{\Delta^2} - \frac{6i\Omega}{\Delta^3} \frac{d\Omega}{dt} \right] - \tilde{c}_0 \tilde{c}_1^* \frac{6i\Omega}{\Delta^3} \frac{d\Omega}{dt} . \end{aligned} \tag{A24}$$

Grouping coefficients of $\tilde{c}_0^* \tilde{c}_1$ and using the complex conjugate of the resulting equation to eliminate $\tilde{c}_0 \tilde{c}_1^*$ gives

$$\begin{aligned} & \tilde{c}_0^* \tilde{c}_1 \left[1+\frac{4\Omega^2}{\Delta^2} \right]^2 \\ & \quad \approx Z_{(3)} \left[\frac{\Omega}{\Delta} \left[1+\frac{4\Omega^2}{\Delta^2} \right]^2 - \left[\frac{1}{\Delta^3} \frac{d^2\Omega}{dt^2} + \frac{i}{\Delta^2} \frac{d\Omega}{dt} \right] \right. \\ & \qquad \left. \times \left[1+\frac{4\Omega^2}{\Delta^2} \right] + \frac{12\Omega}{\Delta^5} \left[\frac{d\Omega}{dt} \right]^2 \right] . \end{aligned} \tag{A25}$$

Multiplying by the complex-conjugate equation and by 4, expanding Z^2 in terms of the Schrödinger probability amplitudes and adding it to both sides of the resulting equation, making the approximation $Z \approx Z_{(3)}$, and solving for $Z_{(3)}$ yields

$$\begin{aligned} Z_{(3)} \approx \pm \left| \frac{\Delta}{\Omega'} \right| & \left[1+\frac{4\Delta^2}{\Omega'^6} \left[\frac{d\Omega}{dt} \right]^2 + \frac{96\Omega^2}{\Omega'^6} \left[\frac{d\Omega}{dt} \right]^2 \right. \\ & - \frac{96\Omega}{\Omega'^8} \left[\frac{d\Omega}{dt} \right]^2 \frac{d^2\Omega}{dt^2} - \frac{8\Omega}{\Omega'^4} \frac{d^2\Omega}{dt^2} \\ & \left. + \frac{4}{\Omega'^6} \left[\frac{d^2\Omega}{dt^2} \right]^2 + \frac{576\Omega^2}{\Omega'^{10}} \left[\frac{d\Omega}{dt} \right]^4 \right]^{-1/2} . \end{aligned} \tag{A26}$$

The third-order polarization

$$\begin{aligned} P_{(3)} = 2iN\mu Z_{(3)} & \left[\frac{\Omega}{\Delta} + \frac{12\Omega}{\Delta\Omega'^4} \left[\frac{d\Omega}{dt} \right]^2 - \frac{1}{\Delta\Omega'^2} \frac{d^2\Omega}{dt^2} \right. \\ & \left. - \frac{i}{\Omega'^2} \frac{d\Omega}{dt} \right] \end{aligned} \tag{A27}$$

is obtained from Eq. (A25).

While each order of approximation can be derived independently by the techniques presented here, it is convenient to begin with the expression for $\tilde{c}_0^* \tilde{c}_1$ from the previous order and add the next term in the expansion. This is permissible because the derivatives of Z were used to approximate the derivates of $Z_{(n)}$. Therefore we replace $Z_{(3)}$ by $Z_{(4)}$ in Eq. (A27), divide by $2iN\mu$, and add the fourth term (A7) in the expansion (A1) to get

$$\begin{aligned} \tilde{c}_0^* \tilde{c}_1 \approx Z_{(4)} & \left[\frac{\Omega}{\Delta} + \frac{12\Omega}{\Delta\Omega'^4} \left[\frac{d\Omega}{dt} \right]^2 - \frac{1}{\Delta\Omega'^2} \frac{d^2\Omega}{dt^2} \right. \\ & \left. - \frac{i}{\Omega'^2} \frac{d\Omega}{dt} + iA \right] \\ & + \tilde{c}_0^* \tilde{c}_1 (-B+iC) + \tilde{c}_0 \tilde{c}_1^* (B+iC) . \end{aligned} \tag{A28}$$

To simplify the algebra we define the temporary variables

$$\Gamma = \frac{\Omega}{\Delta} + \frac{12\Omega}{\Delta\Omega'^4} \left[\frac{d\Omega}{dt} \right]^2 - \frac{1}{\Delta\Omega'^2} \frac{d^2\Omega}{dt^2} \tag{A29}$$

and

$$\Xi = -\frac{1}{\Omega'^2} \frac{d\Omega}{dt} + A . \tag{A30}$$

The approximate inversion and polarization are obtained by the same manipulations as before, with the results

$$Z_{(4)} \approx \pm \left[1+4\Gamma^2+4 \left[\frac{\Xi+2\Gamma C}{1+2B} \right]^2 \right]^{-1/2} \tag{A31}$$

and

$$P_{(4)} \approx 2iN\mu Z_{(4)} \left[\Gamma + i \frac{\Xi+2\Gamma C}{1+2B} \right] . \tag{A32}$$

For the fifth-order approximation we define the additional temporary variable

$$\Lambda = \frac{\Xi+2\Gamma C}{1+2B} . \tag{A33}$$

The approximate inversion and polarization are obtained by the same manipulations as before, with the results

$$Z_{(5)} \approx \pm \left[1+4\Lambda^2+4 \left[\frac{D+\Gamma-2G\Lambda}{1-2F} \right]^2 \right]^{-1/2} \tag{A34}$$

and

$$P_{(5)}=2iN\mu Z_{(5)}\left[\frac{D+\Gamma-2G\Lambda}{1-2F}+i\Lambda\right]. \tag{A35}$$

The method of approximation for the real field can be generalized to a complex field, with the results

$$Z_{(1)}\approx\pm\frac{1}{\left[1+\frac{4|\Omega|^2}{\Delta^2}\right]^{1/2}}=\pm\left|\frac{\Delta}{\Omega'}\right|, \tag{A36}$$

$$P_{(1)}=\frac{2iN\mu\Omega Z_{(1)}}{\Delta}, \tag{A37}$$

$$Z_{(2)}\approx\pm\left|\frac{\Delta}{\Omega'}\right|\left[\left[1+\frac{4\Delta^2}{\Omega'^6}\frac{d\Omega}{dt}\frac{d\Omega^*}{dt}-\left[\frac{8\Delta^2+16|\Omega|^2}{\Delta^2\Omega'^6}\right]\times\left[\Omega\frac{d\Omega^*}{dt}-\Omega^*\frac{d\Omega}{dt}\right]^2+\frac{4i}{\Delta\Omega'^2}\left[\Omega\frac{d\Omega^*}{dt}-\Omega^*\frac{d\Omega}{dt}\right]\right]^{-1/2}, \tag{A38}$$

and

$$P_{(2)}=2iN\mu Z_{(2)}\left\{\frac{\Omega}{\Delta}-i\left[\frac{1}{\Omega'^2}\frac{d\Omega}{dt}-\frac{2\Omega}{\Delta^2\Omega'^2}\left[\Omega\frac{d\Omega^*}{dt}-\Omega^*\frac{d\Omega}{dt}\right]\right]\right\}, \tag{A39}$$

where Ω' is the generalized Rabi frequency for a complex field, $\Omega'(t)=[\Delta^2+4|\Omega(t)|^2]^{1/2}$. The term $\Omega\,d\Omega^*/dt-\Omega^*d\Omega/dt$ is purely imaginary and can be a significant portion of the approximation for self-phase modulated pulses, especially if the Rabi frequency is large and/or if the detuning is small.

APPENDIX B

The graphical results can be applied to related problems and physical understanding can be enhanced by scaling Schrödinger's equation. Define a dimensionless time $\tau=t\tau_p$ and a dimensionless field $\varepsilon=\mu E\tau_p/2\hbar$, where τ_p is a characteristic pulse time. Equations (1) and (2) become

$$\frac{\partial\bar{c}_0}{\partial\tau}=i\varepsilon^*\bar{c}_1, \tag{B1}$$

$$\frac{\partial\bar{c}_1}{\partial\tau}=i\Delta\tau_p\bar{c}_1+i\varepsilon\bar{c}_0, \tag{B2}$$

respectively. Equations (B1) and (B2) show that when the problem is stated in terms of the dimensionless independent variable τ, the answer is completely determined by the dimensionless constants (i) $\mu E_0\tau_p/2\hbar$ and (ii) $\Delta\tau_p$ for the same form of pulse envelope. The polarization resulting from the solution to (B1) and (B2) then scales as $N\mu$. Condition (i), requiring a constant pulse area, and condition (ii), which requires that the angular motion of the pseudodipole about the effective field in a coordinate system rotating with the effective field also remain constant, can be combined to obtain other constant, dimensionless relationships; (iii) $\mu E_0/\Delta\hbar$ and

$$\text{(iv)}\ \frac{\Omega'}{\Delta}=\left[1+\left[\frac{\mu E_0}{\Delta\hbar}\right]^2\right]^{1/2}.$$

Conditions (iii) and (iv) require that the Rabi frequency and the generalized Rabi frequency scaled by the detuning frequency remain constant. Thus all frequencies maintain a constant relationship to one another.

[1] G. L. Peterson and C. D. Cantrell, Phys. Rev. A **31**, 807 (1985).

[2] A. Messiah, *Quantum Mechanics* (North-Holland, Amsterdam, 1962), Vol. II, pp. 749–751.

[3] M. D. Crisp, Phys. Rev. A **8**, 2128 (1973).

[4] M. E. Crenshaw and C. D. Cantrell, Opt. Lett. (to be published); preliminary results on laser propagation in a vapor of two-level systems, including a full treatment of diffraction and making use of the time-dependent Schrödinger equation instead of the steady-state approximation, have been presented by M. E. Crenshaw, C. D. Cantrell, C. A. Glosson, and D. D. Chu, in *Science and Engineering on Cray Supercomputers*, Proceedings of the Third International Symposium, Minneapolis, 1987, edited by J. E. Aldag (Cray Research, Inc., Minneapolis, MN, 1987), pp. 477–490.

[5] D. Grischkowsky, Phys. Rev. Lett. **24**, 866 (1970).

[6] D. Grischkowsky and J. A. Armstrong, Phys. Rev. A **6**, 1566 (1972).

[7] D. Grischkowsky, E. Courtens, and J. A. Armstrong, Phys. Rev. Lett. **31**, 422 (1973).

[8] D. Grischkowsky, in *Laser Applications to Optics and Spectroscopy*, edited by S. F. Jacobs, M. Sargent III, J. F. Scott, and M. O. Scully (Addison-Wesley, Reading, MA, 1975), pp. 437–452.

[9] D. Grischkowsky, Phys. Rev. A **7**, 2096 (1973).

[10] C. D. Cantrell, F. Rebentrost, and W. H. Louisell, Opt. Commun. **36**, 303 (1981).

[11] S. L. McCall and E. L. Hahn, Phys. Rev. **183**, 457 (1969); S. L. McCall and E. L. Hahn, Phys. Rev. Lett. **18**, 908 (1967).

[12] I. S. Gradshteyn and I. M. Ryzhik, *Table of Integrals, Series, and Products* (Academic, New York, 1980), p. 307.

[13]*Higher Transcendental Functions,* edited by A. Erdélyi (Krieger, Malabar, FL, 1985), Vol. II, Chap. VIII.
[14]*Handbook of Mathematical Functions,* edited by M. Abramowitz and I. A. Stegun (Dover, New York, 1972), Chap. 7.
[15]The complementary error function of complex argument was evaluated using the IMSL Library subroutine MERRCZ, IMSL, Inc., Houston, TX (1982).
[16]*Higher Transcendental Functions,* edited by A. Erdélyi (Krieger, Malabar, FL, 1985), Vol. I, Chap. II.
[17]D. D. Chu and C. D. Cantrell (unpublished).
[18]D. J. Kaup, Phys. Rev. A **16**, 704 (1977).
[19]L. Allen and J. H. Eberly, *Optical Resonance and Two-Level Atoms* (Wiley, New York, 1975), pp. 72–77.